50. Lechner, R. B., Gurll, N. J. and Reynold, D. G., *Am. J. Physiol.*, 1986, **249**, H272.
51. Machuganska, A. and Zaharieva, S., *Acta. Physiol. Pharmacol. Bulg.*, 1985, **11**, 34.
52. Gurll, N. J., Gamus, E. and Reynolds, D. G., *Circ. Shock*, 1987, **22**, 115.
53. Houck, C. R., *Am. J. Physiol.*, 1951, **167**, 523.
54. Mitchel, G. A. G., *Acta. Anat.*, 1957, **13**, 1.
55. Brown, J. J., Davis, D. L., Lever, A. F., Parker, R. A. and Robertson, J. I. S., *Lancet*, 1963, **2**, 668.
56. Monta, H. and Vatner, S. F., *Circ. Shock*, 1983, **10**, 317.
57. Skoog, P. J., Manson, and Thoren, P., *Acta. Physiol. Scand.*, 1985, **125**, 655.
58. Morita, H., Manders, W. T. and Vatner, S. F., *Circulation*, 1985, **72**, 111.
59. Lechner, R. B., Gurll, N. J. and Reynold,D. G., *Proc. Soc. Exp. Biol. Med.*, 1985, **178**, 227.
60. Matheyse, F. J. and Engelbrecht, F. M., *Circ. Shock*, 1986, **19**, 385.

Compressional wave velocity–density relationships for the metamorphic rocks of South Indian granulite terrain

C. Ramachandran

Geological Survey of India, 323-CMH Road, Indiranagar, Bangalore 560 038, India

The relationship between compressional (P) wave velocity and density of rock is important in interpretation of gravimetric and seismic data. This relationship has not so far been studied for the South Indian granulite terrain (SGT), which exposes one of the largest high-grade gneiss–charnockite terrains of the world. I have obtained P-wave velocity and density data for the metamorphic rocks of SGT. The velocity–density relationship shows distinct trends for charnockites and gneisses. This may be attributed to differences in the complex metamorphic histories of the two major rock types. The charnockites are the result of varying prograde metamorphic conditions, while the gneisses are mostly the final retrogressed products of charnockites.

WOOLARDS curve[1] and Nafe–Drake curve[2] have been extensively used for estimation of density (ρ) from compressional-wave (P-wave) velocity (V_P) and vice versa. In the present study, I have obtained the $V_P - \rho$ relation for 140 rock samples comprising charnockites, gneisses and amphibolites spread over a traverse length of about 2500 km in SGT. Figure 1 gives the locations of the samples. V_P was measured in core samples using the ultrasonic pulse transmission technique[3] with an overall accuracy of about 2%. Density (ρ) was obtained on dry samples by the standard method of weighing the sample in air and in water using a physical balance. The accuracy of density measurements was $\pm$ 0.005 g cm^{-3}. The wet density would be higher by about 0.01 g cm^{-3}, since even the crystalline rocks have a small porosity at low pressures.

Good examples of different degrees of progressive formation of charnockites from gneisses have been found in Tamil Nadu[4,5] and Kerala[6,7]. Geothermobarometry indicates temperatures of 650–800°C and pressures of 5–9 kbar for the charnockite formation in various parts of SGT[8,9]. Massive influx of CO_2-rich fluids was considered to be responsible for charnockitization in SGT; however, the source of fluids appears to be different for parts of Tamil Nadu and Kerala[10]. The available age data (540–3100 Myr) for SGT indicate polyphase metamorphic history[11]. SGT possibly comprises different tectonic blocks[12,13], welded together during Proterozoic times. Also, initial to intense stages of retrograde metamorphism affected the charnockites of SGT[5,14,15]. Gneisses are generally observed to be the final retrogressed products of charnockites[4,8,14,15]; however, in some areas it is difficult to indicate whether the relations between charnockite and gneiss are prograde or retrogressive[8]. The charnockites and gneisses of SGT were presumably formed by complex metamorphic processes.

V_P depends on petrological composition and rock fa-

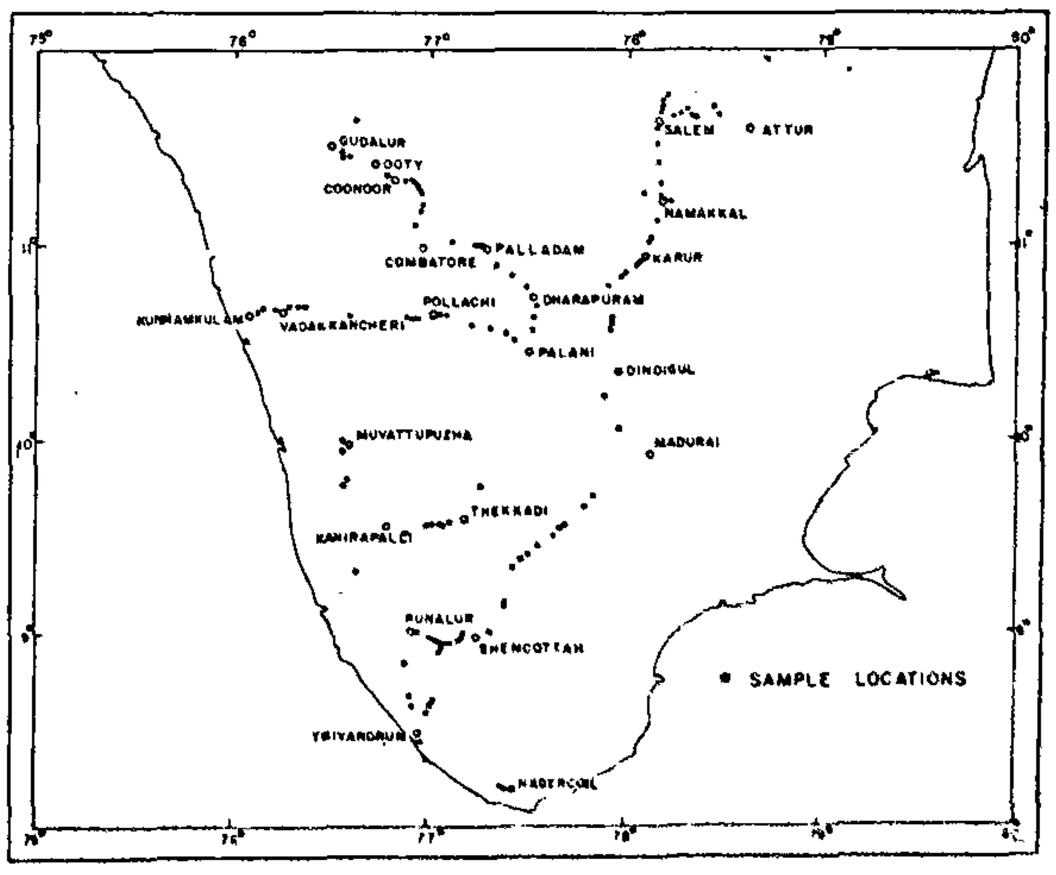

Figure 1. Map showing the locations of samples in the South Indian granulite terrain.

bric and is also influenced by the presence, size and orientation of pores and cracks. The large scatter observed in the $V_P-\rho$ plot (Figure 2) can be mainly attributed to compositional differences due to different metamorphic histories of charnockites and gneisses. Measurements of V_P in two directions, viz. along the axis of the core and along the diameter, show that most of the rocks exhibited velocity anisotropy (0.1–16%), which would also contribute to some scatter in the $V_P-\rho$ plot.

The charnockites were characterized by V_P between 5.0 and 7.38 km s^{-1}, and ρ between 2.6–3.2 g cm^{-3}. Petrographic studies in 54 samples showed that the general composition of charnockites is quartz + feldspar + pyroxene ± biotite ± tremolite ± hornblende ± chlorite ± epidote ± garnet + opaques. It was earlier observed[16,17] that, though the initial stages of retrograde metamorphism in charnockites affected their magnetic properties, the effect is not diagnostic in the case of V_P and ρ. V_Ps of rock-forming minerals were compiled by Gebrande[18] and Christenson and Fountain[19]. Since pyroxenes are characterized by high V_P (7.7–8.08 km s^{-1}), any small change in the percentage of pyroxenes would greatly influence the V_P of charnockites. Some charnockites contain garnet while others are garnet-free, and the presence or absence of garnet (V_P = 8.4–9.3 km s^{-1}; ρ = 4.16 g cm^{-3}) would also contribute to variation of V_P in charnockites. Quartz has a relatively low V_P (6.05 km s^{-1}) and low ρ (2.65 g cm^{-3}) compared to V_P and ρ of the other rock-forming minerals of charnockites, and hence a decrease in quartz content would increase the V_P of charnockites. In general, the basic (mafic) charnockites are characterized by higher velocities than the acid and intermediate charnockites.

Gneisses comprise garnet biotite gneiss, biotite gneiss, granitic biotite gneiss, hornblende biotite gneiss and quartzofeldspathic gneiss. Thin-section studies have indicated that the general composition of gneisses is feldspar + quartz ± hornblende ± garnet ± apatite ± epidote ± calcite + opaques. The scatter in the V_P of gneisses (4.15–6.0 km s^{-1}) is much broader for the limited variation of ρ (2.59–2.87 g cm^{-3}). Both the mean V_P (5.38 km s^{-1}) and ρ (2.73 g cm^{-3}) of gneisses are lower than those of charnockites. Intense retrograde metamorphism of charnockites, culminating in the formation of gneisses, resulted in a mineralogy with a lower aggregate V_P and ρ; particularly, the high-V_P and high-ρ pyroxenes of charnockites are completely altered. Besides, generation of new microcracks due to thermal expansion of mineral grains owing to thermal cycling[18] during retrograde metamorphism may also have contributed to the velocity decrease in gneisses. The presence or absence of garnet in gneisses would contribute significantly to V_P variation: Biotite has low V_P (5.35 km s^{-1}) and high ρ (3.05 g cm^{-3}), and its abundance would decrease V_P while slightly increasing ρ.

The $V_P-\rho$ regression relation ($V_P = 4.85\rho - 7.88$) for gneisses (Figure 2) is similar to that obtained by Gabrande[18] ($V_P = 4.41\rho - 6.93$) for quasi-isotropic metamorphics. The $V_P-\rho$ relation for charnockites ($V_P = 2.0\rho + 0.61$) is similar to that obtained by Christenson and Fountain[19] for 40 samples of granulites ($V_P = 2.27\rho + 0.31$).

The results show that the variation of V_P with ρ in charnockites, which were formed in varying prograde metamorphic conditions, shows a trend different from that of gneisses, which are mostly the retrogressed products of charnockites. Hence a single relationship between V_P and ρ cannot be used for the metamorphics of SGT. The $V_P-\rho$ relations of charnockites and gneisses are dependent in a complex way on their mineralogy and their metamorphic history.

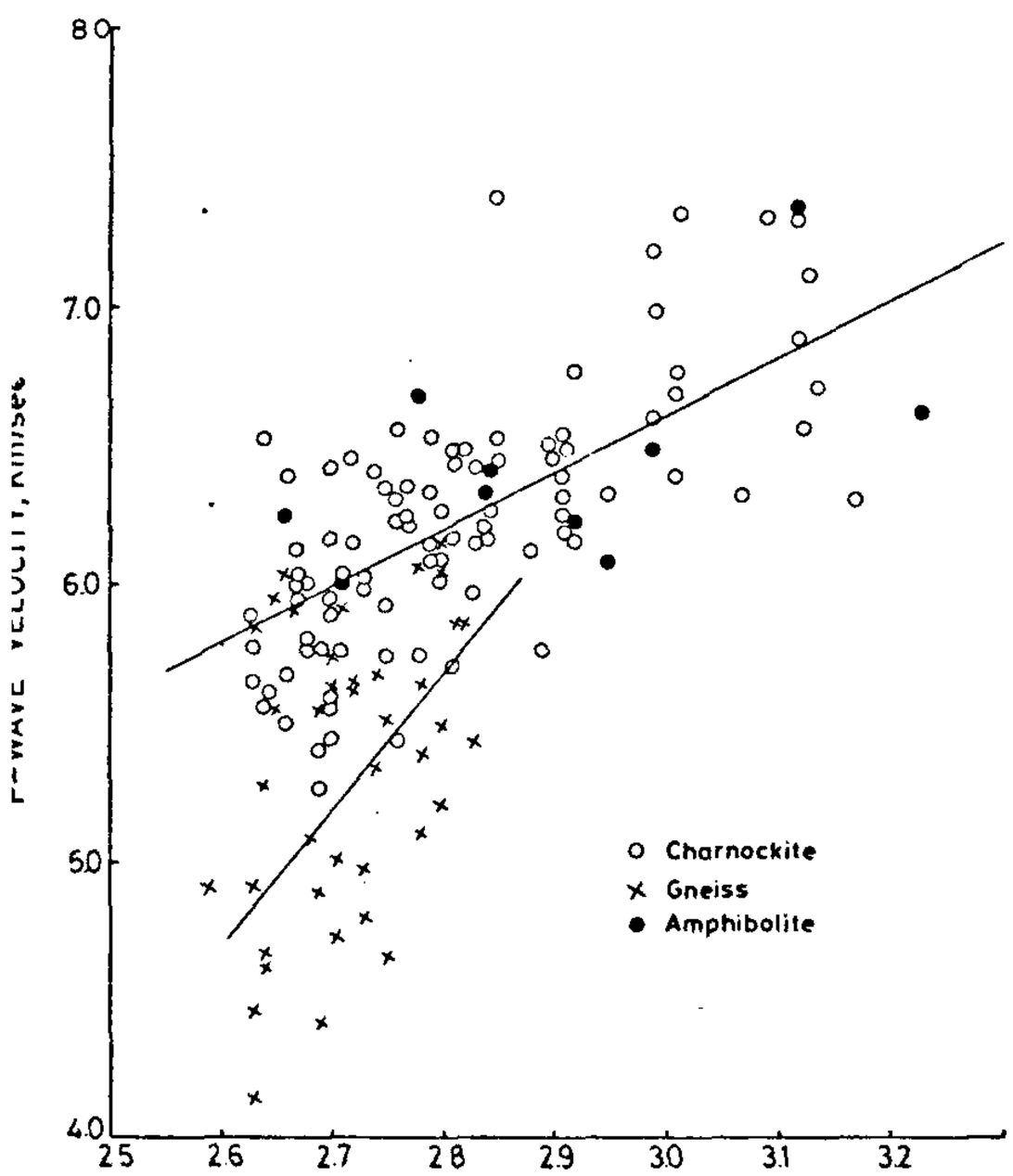

Figure 2. Variation of P-wave velocity with density for the metamorphic rocks of South Indian granulite terrain.

1. Woolard, G. P., *Bur. Grav. Int. Bull. Laf.*, 1975, **36**, 106.
2. Nafe, J. E. and Drake, C., in *The Sea* (ed. Hill, M. N.), Interscience, New York, 1963, vol. 3, p. 794.
3. Ramachandran, C., *Indian Miner.*, 1986, **40**, 1.
4. Allen, P., Kondie, K. C. and Narayana, B. L., *Geochem. Cosmochem. Acta*, 1985, **49**, 323.
5. Janardhan, A. N., Newton, R. C. and Hansen, E. C., *Contrib. Mineral. Petrol.*, 1982, **79**, 130.

6. Ravindrakumar, G. R., Srikantappa, C. and Hansen, E., *Nature*, 1985, **313**, 207.
7. Srikantappa, C., Raith, M. and Spiering, B., *J. Geol. Soc. India*, 1985, **26**, 849.
8. Newton. R. C. and Hansen, E. C., *Geol. Soc. Spl. Publ.*, 1986, no. 24, p. 293.
9. Santosh, M., *Mem. Geol. Soc. India*, 1988, **11**, 91.
10. Newton, R. C., *J. Geol. Soc. India*, 1988, **31**, 103.
11. Ravindrakumar, G. R., *J. Geol. Soc. India*, 1988, **31**, 123.
12. Drury, S. A., Harris, N. B. W., Holt, R. W., Reeves-Smith, G. J. and Wightman, R. T., *J. Geol.*, 1984, **92**, 1.
13. Viswanatha, T. V., Gopalakrishnan, K., Ganeshan, T. M. and Raman, R., in *Group Discussion on 'Suture Zones—Young and Old'*, Geological Survey of India, Calcutta, 1990, p. 47.
14. Yoshida, M. and Santosh, M., *J. Geosci.*, 1987, **30**, 23.
15. Raith, M., Rasse, P., Ackermand, D. and Lal, R. K., *Trans. R. Soc. Edinburgh, Earth Sci.*, 1983, **73**, 221.
16. Ramachandran, C., *J. Geol. Soc. India*, 1990, **35**, 395.
17. Ramachandran, C., *Tectonophysics*, (communicated)
18. Gebrande, H., in *Physical Properties of Rocks*, (ed. Angenheister, G., Springer-Verlag, Berlin, New York, 1982, p. 1–35.
19. Christenson, N. I. and Fountain, D. M., *Geol. Soc. Am. Bull.*, 1975, **86**, 227.

ACKNOWLEDGEMENT. I thank Ms L. R. Bosu and Mr S. S. Dey for assistance during the measurements, and Mr C. Bhattacharya for petrographic studies on 54 samples. Mr Dipak Belur did the regression analysis.

Received 21 August 1990; revised accepted 6 July 1991

Hydrothermal phase relations in molybdenum oxide–water systems

B. Basavalingu and J. A. K. Tareen

Department of Studies in Geology, University of Mysore, Mysore 570 006, India

Molybdenum oxides are important for materials scientists as they show good semiconducting properties. Study of stability relations in molybdenum oxide system is interesting from the point of view of syntheses of pure phases of the oxides or of mixed oxides with other cations. We have studied phase stability in molybdenum oxide–water systems using Tuttle-type pressure vessels. MoO_3 on the low-temperature side and MoO_2 on the high-temperatue side were the stable oxides. A metastable blue phase found between the MoO_3 and MoO_2 fields was a hydrated nonstoichiometric molybdenum oxide.

MOLYBDENUM has tetravalent (MoO_2) and hexavalent (MoO_3) stable oxidation states, but many nonstoichiometric 'magneli' phases with composition MoO_n ($2 < n < 3$) have been reported because of its mixed valence states[1–3]. Preparation of such oxides by high-temperature methods usually involves uncertainty with regard to oxygen stoichiometry, particularly when the process involved is high-temperature sintering with or without control of oxygen fugacity in the atmosphere. One of the promising techniques of synthesis and growth of single crystals of oxides is the hydrothermal method, which has not received extensive attention from materials scientists. We have been studying the phase relations in several transition metal oxide–water systems in steel or stellite reactor vessels under hydrothermal conditions[4–7]. The intrinsic oxygen fugacity developed in steel or stellite reactors with water

Table 1. Experimental details for the H_2MoO_4–H_2O system.

Temp. (°C)	Pressure (bar)	Duration (h.)	Product
175	350	68	$MoO_3 \cdot nH_2O$
200	350	59	$MoO_3 \cdot nH_2O$
225	350	69	$MoO_3 \cdot nH_2O + MoO_2$
300	350	72	MoO_2
400	350	68	MoO_2
150	700	84	$MoO_3 \cdot nH_2O$
200	700	66	$MoO_3 \cdot nH_2O$
250	700	86	MoO_2
350	700	58	MoO_2
450	700	94	MoO_2
550	700	56	MoO_2
150	1050	68	$MoO_3 \cdot nH_2O$
225	1050	86	$MoO_3 \cdot nH_2O$
300	1050	99	MoO_2
400	1050	56	MoO_2
150	1750	78	$MoO_3 \cdot nH_2O$ + *
220	1750	86	$MoO_3 \cdot nH_2O$ + *
350	1750	77	MoO_2 + *
110	2100	85	$MoO_3 \cdot nH_2O$
175	2100	94	$MoO_3 \cdot nH_2O$ + *
250	2100	58	$MoO_3 \cdot nH_2O$ + *
350	2100	58	*
450	2100	69	MoO_2
550	2100	89	MoO_2

*Blue oxide phase

Table 2. Experimental details for the MoO_3–H_2O system.

Temp. (°C)	Pressure (bar)	Duration (h.)	Product
150	350	78	MoO_3
250	350	69	MoO_3
350	350	79	MoO_3
400	350	88	MoO_3
450	350	86	*
500	350	48	MoO_2
600	350	72	MoO_2
675	350	54	MoO_2
750	350	84	MoO_2
400	850	68	* + MoO_3
200	1050	64	MoO_3
300	1050	94	MoO_3 + *
350	1050	69	MoO_3 + *
450	1050	65	*
550	1050	64	*
600	1050	59	MoO_2
700	1050	95	MoO_2
200	1750	85	MoO_3
250	1750	77	MoO_3
300	1750	56	MoO_3 + *
400	1750	78	*
500	1750	88	*
600	1750	73	MoO_2 + *
700	1750	94	MoO_2